Proline Isomerization in Bovine Pancreatic Ribonuclease A. 1. Unfolding Conditions†

D. Juminaga, W. J. Wedemeyer,‡ and H. A. Scheraga*

Baker Laboratory of Chemistry, Cornell University, Ithaca, New York 14853-1301

Received May 5, 1998; Revised Manuscript Received June 26, 1998

ABSTRACT: The slow fluorescence unfolding phase of bovine pancreatic ribonuclease A is studied by stopped-flow kinetics and site-directed mutagenesis of tyrosines to phenylalanine and prolines to alanine. It is shown conclusively that this phase arises from *two* specific sources: Tyr92 reporting on the *cis*−*trans* isomerization of Pro93 and Tyr115 reporting on the *cis*−*trans* isomerization of Pro114. Previous studies have conjectured that the slow unfolding phase arises from only *one* source (Tyr92-Pro93 *cis*−*trans* isomerization) based primarily on studies of the homologous protein guinea pig ribonuclease A [Schmid, F. X., Grafl, R., Wrba, A., and Beintema, J. J. (1986) *Proc. Natl. Acad. Sci. U.S.A. 83*, 872−876]; it is proposed here that Lys113 in the latter protein interferes with the isomerization of the Lys113-Pro114 peptide group. The site-directed mutations studied here enable the *individual* isomerizations of Pro93 and Pro114 to be monitored, providing an optical technique by which these well-defined molecular folding events can be studied, under both folding and unfolding conditions, and compared to molecular simulations. The time constants for Pro93 and Pro114 isomerization agree closely with those of our box model of proline isomerization under unfolding conditions, which had been derived from exhaustive statistical modeling of double-jump refolding data [Juminaga, D., Wedemeyer, W. J., Garduño-Júarez, R., McDonald, M. A., and Scheraga, H. A. (1997) *Biochemistry 36*, 10131−10145].

Proline isomerization during protein folding has been actively studied for over 2 decades (*1*, *2*). Since proline is an *imino* acid, its X-Pro peptide group has *trans* and *cis* isomers of nearly equal energy (*3*). The relative populations of these isomers are roughly 3:1 (*trans*:*cis*) in small peptides and unfolded proteins (*4*), although the precise ratio varies with the preceding amino acid. By contrast, the ratio for the *amino* acids is greater than 100:1 (*3*, *5*, *6*). When an unfolded protein is exposed to folding conditions, its prolines generally adopt a single isomeric state, although a few proteins exhibit isomeric heterogeneity even in the native state (*7*).

The isomeric state of some proline residues can profoundly affect the conformational refolding of the whole protein (*1*); such prolines are termed "essential" (*8*). Nevertheless, conformational folding generally precedes isomerization to the native isomer. In other words, non-native isomers decelerate, but generally do not block, conformational refolding (*9*).

Bovine pancreatic ribonuclease A (RNase A[1]) has long been a test system for studying the relationship between proline isomerization and conformational folding (for a recent review, see ref *10*). The refolding of RNase A is heterogeneous, and five exponential phases have been detected by tyrosine absorbance; these phases are denoted U_{vf}, U_f, U_m, U_S^{II}, and U_S^{I}, representing the very fast, fast, medium, major slow, and minor slow refolding phases. RNase A (*11*, *12*; Figure 1) has four prolines (*trans*-Pro42, *cis*-Pro93, *cis*-Pro114, and *trans*-Pro117), of which the latter three are essential (*13*). Using exhaustive statistical fitting of double-jump refolding data, a new "box" model has been derived to describe the relationship between the five conformational refolding phases of RNase A and the eight isomeric states of its three essential prolines under unfolding conditions (*14*). This paper measures the isomerization kinetics of Pro93 and Pro114 under unfolding conditions, and the observed time constants agree with those derived from the box model.

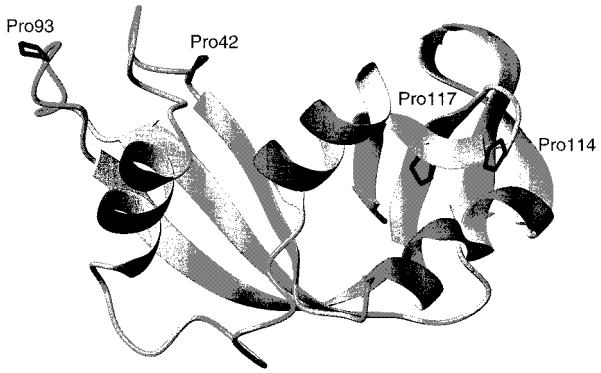

FIGURE 1: Ribbon diagram of RNase A with the four prolines indicated. The structure was taken from Wlodawer et al. (*11*). The diagram was prepared with the program MOLMOL of Koradi et al. (*12*).

† This work was supported by Grant No. GM-24893 from the National Institute of General Medical Sciences of the National Institutes of Health. Support was also received from the National Foundation for Cancer Research.

* To whom correspondence should be addressed.

‡ NIH Trainee, 1993−1996.

[1] Abbreviations: RNase A, disulfide-intact bovine pancreatic ribonuclease A; cCMP, cytidine 2′:3′-cyclic monophosphate; Gdn·HCl, guanidine hydrochloride; Gdn·SCN, guanidine thiocyanate; NTB, 2-nitro-5-thiobenzoate; NTSB, disodium 2-nitro-5-thiosulfobenzoate.

S0006-2960(98)01028-9 CCC: $15.00
Published on Web 07/30/1998

When observed by fluorescence under *strong* unfolding conditions (*high* [Gdn·HCl] and *low* pH), RNase A exhibits two phases, a slow phase ($\tau \sim$ min) and a fast phase ($\tau \sim$ ms) (*15*). The fast phase is sensitive to pH and [Gdn·HCl] and is also observed by absorbance, corresponding to the exposure of buried tyrosines to the solvent and, thus, to *conformational* unfolding (*14*). By contrast, the slow phase cannot be observed by absorbance, suggesting that it corresponds to a *localized* process after conformational unfolding (*15*). Moreover, the slow phase is relatively independent of pH and [Gdn·HCl] and has an activation energy of ~20 kcal/mol, suggesting that this phase arises from *cis*−*trans* proline isomerization which reduces the fluorescence quenching of *adjacent* tyrosines (*1*, *15*, *16*). The main goal of this paper is to identify the prolines and tyrosines that are responsible for the slow fluorescence unfolding phase.

It has long been believed that the slow fluorescence unfolding phase arises from a *single* source, namely, Tyr92 reporting on the isomerization of Pro93 (*15*, *16*). If true, the amplitude of this phase could be used as a specific assay of the isomeric state of Pro93 (*17*−*19*). However, kinetic studies of the slow unfolding fluorescence phase of the site-directed mutant Y92F have cast doubt on this interpretation (*14*).

In this paper, further kinetic studies of the fluorescence-monitored unfolding of several new site-directed mutants demonstrate that the slow fluorescence unfolding phase arises from *two* sources, specifically from Tyr92 reporting on Pro93 and from Tyr115 reporting on Pro114. The site-directed mutants enable us to track the *individual* isomerizations of Pro93 and Pro114 under unfolding and folding conditions, and the observed rate constants agree with those of the proposed "box" model (*14*). The ability to follow individual proline isomerizations optically provides a new avenue into the conformational folding of proteins and yields definitive results against which molecular simulations can be compared.

MATERIALS AND METHODS

Purification of Wild-Type Ribonuclease A. Wild-type bovine pancreatic ribonuclease A type 1-A (Sigma) was purified by cation-exchange chromatography according to the procedure of Rothwarf and Scheraga (*20*).

Expression and Purification of Mutants. The mutant plasmids for Y92F, P42A, P93A, P114A, and P117A[2] were obtained from previous studies (*13*, *14*). For Y115F, the mutation was carried out with the synthetic gene for bovine pancreatic ribonuclease A (a gift from the Genex Corp.), which was originally cloned in an M13mp18 vector (United States Biochemical) but later transferred into the pET22b-(+) vector (Novagen) between the *Msc*I and *Hind*III restriction enzyme sites following the procedures described previously (*14*). The codon corresponding to Tyr115 was mutated to TTT (phenylalanine) to obtain the Y115F mutant. For the double mutants [Y92F/Y115F] and [Y92F/P114A], the Y92F cDNA in pET22b(+) from the previous study was used. The codons for Tyr115 and Pro114 were changed to TTT (phenylalanine) and GCT (alanine), respectively. The procedures for site-directed mutagenesis followed the Kunkel method (*21*).

The procedures for the expression and purification of the mutant proteins were described previously (*13*). The correctness of the mutations was confirmed by DNA sequencing, amino acid analysis, and mass spectrometry.

Determination of Extinction Coefficient. For the wild-type protein and the Y92F, P42A, P93A, P114A, and P117A mutants, their extinction coefficients were obtained from previous studies (*13*, *14*). For the new mutants, the extinction coefficients were determined by means of an NTSB assay for disulfides (*22*). The absorbances of approximately 1 mg/mL of the protein stock solutions (in 100 mM acetic acid) were measured at 275 nm. The NTSB assay was carried out by mixing 60 μL of the protein stock solution with 1220 μL of the assay buffer (2 M Gdn·SCN, 50 mM glycine, 300 mM sodium sulfite, 3 mM EDTA, 25 mM NTSB, pH 9.5). The formation of NTB was followed by measuring the absorption at 412 nm, and the concentration of NTB formed was determined using 13 900 M^{-1} cm^{-1} as the molar extinction coefficient of NTB at 412 nm (*22*). The resulting concentration of NTB was then used to calculate the concentration of the protein stock solution and, hence, the molar extinction coefficients of the proteins at 275 nm. All of the absorption measurements were carried out with a modified Cary model 14 spectrophotometer (*23*).

Determination of Enzymatic Activity. The enzymatic activities were determined from the catalytic rate of hydrolysis of cytidine 2′:3′-cyclic monophosphate (cCMP) (Sigma) in 100 mM Tris, 0.2 M NaCl, pH 7, at room temperature (*24*). The rates of catalysis were monitored by absorption at 286 nm and the slopes (Δabsorbance/Δtime) divided by the concentrations of the wild-type protein, and the mutants were compared. The relative rates of catalysis are reported as percentages of the wild-type rate.

Guanidine Hydrochloride Transitions. A series of solutions with the protein (~1 mg/mL) dissolved in 0.1 M sodium acetate, pH 5.0, at various concentrations of Gdn·HCl, was allowed to equilibrate at 15 °C overnight. Gdn·HCl concentrations were determined by measuring refractive indices of the solutions at 25 °C (*25*) using a Bausch and Lomb refractometer. Absorbance at 287 nm was measured with a modified Cary model 14 spectrophotometer (*23*) with the sample compartments maintained at 15 °C. The transitions were analyzed by the method described by Santoro and Bolen (*26*).

Single-Jump Stopped-Flow Kinetic Experiments. All of the kinetic data presented in this paper were determined by fluorescence measurements. The experimental setup, using a Hi-Tech PQ/SF-53 stopped-flow apparatus, has been described previously (*27*). The flow cell had a path length of 10 mm and a width of 2 mm. A xenon arc lamp (Ushio, Japan) was used as the light source; the excitation wavelength was set at 268 nm, and a band-pass filter (280−400 nm) was used for emission. Data were collected every 0.5 ms for the first minute and every 50 ms thereafter, for 15−20 min. Some experiments (unfolding at 4.2 M Gdn·HCl, pH 2.0, and 15 °C) were repeated by absorption, but the data

[2] Y25F, Y92F, Y97F, and Y115F are the tyrosine-to-phenylalanine mutants of RNase A, corresponding to tyrosines 25, 92, 97, and 115, respectively; P42A, P93A, P114A, and P117A are the proline-to-alanine mutants of RNase A, corresponding to prolines 42, 93, 114, and 117, respectively; [Y92F/Y115F] and [Y92F/P114A] are the mutants of RNase A with two-point mutations consisting of Y92F, Y115F and Y92F, P114A mutations, respectively; α_f, τ_f and α_S, τ_S are the amplitudes and time constants corresponding to the fast and slow unfolding phases, respectively.

Table 1. Summary of the Equilibrium Properties and Enzymatic Activities[a]

	ϵ_{275}[b]	$[Gdn·HCl]_{1/2}$[c]	m[c]	% activity[d]
wild-type	9609 ± 117	3.03	3.72	100
Y92F	8200 ± 120	3.05	2.90	90
P93A	11770 ± 400	2.20	2.79	69
Y115F	7900 ± 130	3.22	3.20	87
P114A	10800 ± 200	2.18	4.40	82
P42A	9900 ± 200	3.02	2.42	57
P117A	10000 ± 200	2.52	2.66	83
[Y92F/Y115F]	6700 ± 85	3.23	2.64	90
[Y92F/P114A]	8000 ± 65	2.28	4.30	95

[a] The data for the Y115F, [Y92F/Y115F], and [Y92F/P114A] are newly obtained in this study, while the data for the wild-type protein and the Y92F, P42A, P93A, P114A, and P117A mutants were obtained from previous studies (*13*, *14*). [b] Molar extinction coefficients (M^{-1} cm^{-1}) at 275 nm (22 °C) in 100 mM acetic acid. [c] $[Gdn·HCl]_{1/2}$ represents the midpoint for the Gdn·HCl transition at 15 °C in 100 mM sodium acetate, pH 5.0, determined by the method of Santoro and Bolen (*26*). m represents the first derivative of the free energy difference between the folded and unfolded states with respect to the concentration of Gdn·HCl. The units for $[Gdn·HCl]_{1/2}$ and m are M and kcal mol^{-1} M^{-1}, repectively. [d] Relative rates for the hydrolysis of cCMP reported as percent of the wild-type rate. The rates refer to the initial slopes of the plots of absorbance at 287 nm, corresponding to the production of the substrate, versus time, at 25 °C in 100 mM acetic acid, pH 7.0.

were not presented. The absorption measurements detected only fast phases whose time constants were similar to those determined by fluorescence. For the absorption measurements, a deuterium lamp (Hellma) was used as a light source, and the monochromator for the incident light was set at 287 nm.

For the single-jump unfolding experiment at 4.2 M Gdn·HCl and pH 2.0, the protein solution in 1.2 M Gdn·HCl, 50 mM sodium acetate at pH 5.0 was mixed (1:10) with the unfolding buffer, 4.5 M Gdn·HCl, 50 mM glycine at pH 1.8; for the unfolding at 5.2 M Gdn·HCl and pH 1.0, a similar protein solution was mixed (1:10) with the unfolding buffer, 5.6 M Gdn·HCl, 120 mM glycine at pH 0.8. The starting protein concentration for all measurements was ~350 μM. Most measurements were carried out at 15 °C. However, to determine the activation energy for the slow phase, measurements were repeated at different temperatures.

Data obtained from all stopped-flow measurements were fit to a sum of exponentials plus a constant baseline and a linear slope to model slight drifts in lamp intensity and photobleaching effects. The fitting was done with a package developed in our laboratory, which employs a simulated annealing Nelder−Mead simplex algorithm (*28*) to minimize the χ^2 statistic. In all cases, the fits were robust and reproducible. Each run was fit and checked individually; the variances of the reported amplitudes and time constants were calculated from the expression $(n - 1)^{-1} \sum(y - \bar{y})^2$, where y is the fitted value of the amplitude or time constant, $\bar{y}$ is the average value, and n is the number of runs. All errors are listed at the 95% confidence limit.

RESULTS AND DISCUSSION

Equilibrium Properties. The equilibrium properties of several new mutants are listed in Table 1. All the mutants have native-like enzymatic activity indicating that their folded conformations are similar to that of the wild-type protein. The relatively large change in the activity of the P42A mutant is presumably due to its effect on the catalytically essential residue Lys41 (*11*). The equilibrium Gdn·HCl transitions show that all the mutants are fully folded (unfolded) under the initial (final) conditions used in our single-jump stopped-flow experiments.

The equilibrium Gdn·HCl transitions show other interesting features. By comparing the wild-type protein with the Y92F mutant, as well as the two pairs of mutants Y115F/[Y92F/Y115F] and P114A/[Y92F/P114A], it is clear that tyrosine 92 does not alter the transition midpoint significantly (Table 1). The Y115F mutation seems to *increase* the transition midpoint slightly, judging from the Y115F mutant compared to the wild-type protein and from the [Y92F/Y115F] mutant compared to the Y92F mutant (Table 1). By contrast, the proline mutants P93A, P114A, and P117A feature strongly depressed transition midpoints (Table 1). This is not surprising; the P114A mutation disrupts the native structure of residues 110−118 of the hydrophobic core, replacing the native *cis* isomer of Pro114 by a *trans* isomer (*29*). Similarly, the P93A mutation causes disorder in the region of residues 89−94, and experiments have indicated that the Tyr92-Ala93 peptide group may remain *cis* in the folded state (*13*, *30*). Pro117 is completely buried in the hydrophobic core (*31*), and hence, its replacement by alanine is likely to disrupt the hydrophobic core. It is interesting to note that the mutation P114A makes the transition *more* cooperative (larger m value), whereas the other mutations make the transition *less* cooperative (Table 1). Finally, the P42A mutation does not affect the transition midpoint significantly (Table 1).

The Reporting Tyrosines. The main goal of this paper is to identify the prolines and tyrosines that are involved in the slow fluorescence unfolding phase. The reporting tyrosines were identified by mutating several tyrosines of RNase A[3] to phenylalanine. This mutation is conservative, eliminating only one atom, the O^{η} atom; nevertheless, the fluorescence properties of the aromatic ring are sufficiently altered to *eliminate* the normal tyrosine fluorescence signal. This approach has the advantage that the mutated residue is *not* observed, except by omission, and thus, a more faithful picture of the wild-type kinetics can be discerned from the fluorescence of the *remaining* tyrosines. This contrasts with our previous approach, exemplified in the Y92W mutant (*32*), where the mutated residue itself is observed and the local dynamics may differ from that of the wild-type protein.

Several tyrosine-to-phenylalanine mutants (Y25F, Y92F, and Y97F) have been described in a previous paper (*14*). In this paper, we consider these mutants as well as the single mutant Y115F and the double mutants [Y92F/Y115F] and [Y92F/P114A]. Judging from their high residual enzymatic activity and thermodynamic parameters (Table 1), these mutants are structurally similar to the wild-type protein, and their proline isomerizations, especially under unfolding conditions, should not be drastically altered. Thus, the contribution of the mutated tyrosines can be selectively "knocked out" without changing the underlying proline isomerizations. It should be noted that no slow phase was

[3] RNase A refers to disulfide-intact bovine pancreatic ribonuclease A; the wild-type protein corresponds to the natural (not recombinant) RNase A.

Table 2. Kinetic Data from the Single-Jump Unfolding at 4.2 M Gdn·HCl, pH 2.0, and 15 °C[a]

	fast phase		slow phase			
	$\bar{\alpha}_f$[b,c]	τ_f (ms)[b,c]	$\bar{\alpha}_S$[b]	τ_S (s)[b]	R_f[d]	R_S[d]
wild-type	0.66	42 ± 1	0.34	74 ± 1	100	100
Y92F	0.75	43 ± 1	0.25	44 ± 1	83 ± 2	54 ± 3
P93A	0.67	41 ± 5	0.33	47 ± 2	61 ± 3	57 ± 2
Y115F	0.67	43 ± 4	0.33	105 ± 2	55 ± 1	54 ± 2
P114A	0.78	26 ± 1	0.22	115 ± 6	68 ± 2	53 ± 3
P42A	0.70	32 ± 1	0.30	73 ± 2	99 ± 2	85 ± 3
P117A	0.67	10 ± 1	0.33	68 ± 1	56 ± 1	69 ± 4
(Y92F+Y115F)[e]	0.73	41 ± 2	0.27	76 ± 2	77 ± 2	54 ± 2
[Y92F/Y115F]	1.00	42 ± 2			43 ± 2	
[Y92F/P114A]	1.00	23 ± 3			69 ± 4	

[a] The single-jump unfolding is from 1.2 M Gdn·HCl, pH 5.0, to 4.2 M Gdn·HCl, pH 2.0, at 15 °C. The unfolding is monitored by fluorescence; the excitation wavelength is 268 nm, and a band-pass filter (280−400 nm) is used for emission. [b] The observed fluorescence increase is fitted to a sum of two exponentials $\{\alpha_f \exp(-t/\tau_f) + \alpha_S \exp(-t/\tau_S)\}$, where α_f and α_S are the amplitudes (in arbitrary units) and τ_f and τ_S are the time constants for the fast (f) and slow (s) phases, respectively. $\bar{\alpha}_f$ and $\bar{\alpha}_S$ correspond to the *normalized* amplitudes, which are calculated using the expressions $\alpha_f/(\alpha_f + \alpha_S)$ and $\alpha_S/(\alpha_f + \alpha_S)$, respectively, so that $\bar{\alpha}_f + \bar{\alpha}_S = 1$. Normalized amplitudes are denoted with bars overhead. [c] The fast unfolding phase is not discussed in this paper; the amplitudes and time constants are included here for completeness. It should be noted that the fast unfolding phase is relatively insensitive to the Y92F, P93A, Y115F, and P42A mutations, as well as the [Y92F/Y115F] double mutation. By contrast, the P114A and P117A mutations significantly accelerate the fast unfolding phase, presumably through their disruptions of the packing of local hydrophobic residues. [d] R_f and R_S represent the ratios of the *unnormalized* amplitudes of the mutants to the wild-type protein. For example, R_S represents α_S divided by $\alpha_{S,WT}$, where these two amplitudes have been corrected for concentration but *not* normalized to their corresponding fast phases (α_f and $\alpha_{f,WT}$). Thus, at identical concentrations, the Y92F, P93A, Y115F, and P114A mutants, as well as the Y92F+Y115F mixture, all have a slow fluorescence phase whose amplitude is roughly one-half that of the wild-type protein ($R_S \approx 0.5$). This correlates well with our model that the slow fluorescence phase in the wild-type protein is the sum of two independent proline isomerizations (at Pro93 and Pro114) being reported by roughly equal fluorescence changes in their adjacent tyrosines (Tyr92 and Tyr115). As described in the text, the proline mutations eliminate the corresponding isomerization, while the tyrosine mutations eliminate the *reporting* of the corresponding isomerization by fluorescence. The P42A and P117A mutations also have smaller slow phase fluorescence amplitudes, which most likely results from changes in the local environments of the tyrosines which in turn affect their fluorescence differences under proline isomerization. The ratio of the fast amplitudes R_f corresponds to changes in *conformational* unfolding which is not discussed in this paper; it is presented here merely for completeness. [e] A 50:50 mixture of Y92F and Y115F at similar concentrations.

detected by absorbance for any of the mutants described in this paper.

The results of these mutational studies on the slow fluorescence unfolding are summarized in Table 2. The mutations Y25F and Y97F produce no effect whatever on the slow fluorescence unfolding, either in the amplitude or in its time constant, as reported in a previous paper (*14*). Hence, Tyr25 and Tyr97 do not appear to contribute to the slow fluorescence unfolding phase, consistent with the assumption that the slow phase is a localized process, since these tyrosines are not adjacent to prolines. Tyr73 and Tyr76 are likewise not adjacent to prolines but conceivably could contribute to the slow fluorescence unfolding phase, through the isomerization of the nearby 65−72 disulfide bridge (*33*). To check this possibility, the double mutant [C65S/C72S], which eliminates this disulfide bridge, was prepared (*34*). The slow fluorescence unfolding phase was not affected significantly (data not shown).

Table 3. Kinetic Data from the Single-Jump Unfolding at 5.2 M Gdn·HCl, pH 1.0, and 15 °C[a]

	fast phase		slow phase	
	$\bar{\alpha}_f$[b]	τ_f (ms)[b]	$\bar{\alpha}_S$[b]	τ_S (s)[b]
wild-type	0.64	11 ± 1	0.36	79 ± 3
Y92F	0.76	9 ± 1	0.24	46 ± 2
P93A	0.66	10 ± 2	0.34	45 ± 2
Y115F	0.69	9 ± 1	0.31	115 ± 3
P114A	0.73	6 ± 1	0.27	114 ± 5

[a] The single-jump unfolding is from 1.2 M Gdn·HCl, pH 5.0, to 5.2 M Gdn·HCl, pH 1.0, at 15 °C. The unfolding is monitored by fluorescence; the excitation wavelength is 268 nm, and a band-pass filter (280−400 nm) is used for emission. [b] See Table 2.

By contrast, the Y92F and Y115F mutations profoundly affect the slow unfolding fluorescence phase. In both mutants, the fluorescence amplitude is reduced by 50%; the time constant observed for Y92F is 44 ± 1 s, whereas that for Y115F is 105 ± 2 s, which are significantly faster and slower, respectively, than that of the wild-type protein (Table 2). The sum of the slow unfolding phases for Y92F and Y115F closely matches that of the wild-type protein. Thus, these two tyrosines (92 and 115) seem to be jointly responsible for the slow unfolding fluorescence phase of RNase A. To verify this observation, the double mutant [Y92F/Y115F] was prepared and, as expected, the slow unfolding fluorescence was completely eliminated (Table 2).

The time constants of the Y92F and Y115F mutants differ almost 3-fold. This raises the question of whether the two phases should not be discernible in the slow unfolding fluorescence phase of wild-type RNase A, where only one exponential phase has ever been reported (*15*−*19*). To address this concern, we repeated our stopped-flow experiments on a 50−50% mixture of the Y92F and Y115F mutants. Only a single exponential could be discerned, and its time constant matched that of wild-type RNase A (Table 2).

The slow phases reported by Tyr92 and Tyr115 bear all the hallmarks of proline isomerization. These fluorescence phases occur on the correct time scale (*4*) and are insensitive to pH and denaturant (Table 3). By contrast, the time constant for the conformational unfolding in the fast phase (in which proline isomerization is *not* involved) is reduced at the higher Gdn·HCl concentration. The activation energies for the slow fluorescence unfolding phases of Y92F and Y115F were measured to be 20.6 ± 0.4 and 20.8 ± 0.3 kcal/mol, respectively, which are consistent with proline isomerization (*1*, *4*). Moreover, the time constants for these two mutants differ significantly from each other under all experimental conditions, indicating that these tyrosines are reporting on the isomerizations of two distinct prolines (Figure 2). This result is not surprising, since these tyrosines are well-separated along the polypeptide chain and, by the locality assumption, the tyrosines should report only the isomerization of prolines adjacent in the sequence.

The Isomerizing Prolines. Proline-to-alanine mutants were prepared for each of the four prolines of RNase A (*13*). Since the *cis*−*trans* ratio for alanine is negligibly small (*3*, *5*, *6*), individual isomerization processes can be selectively "knocked

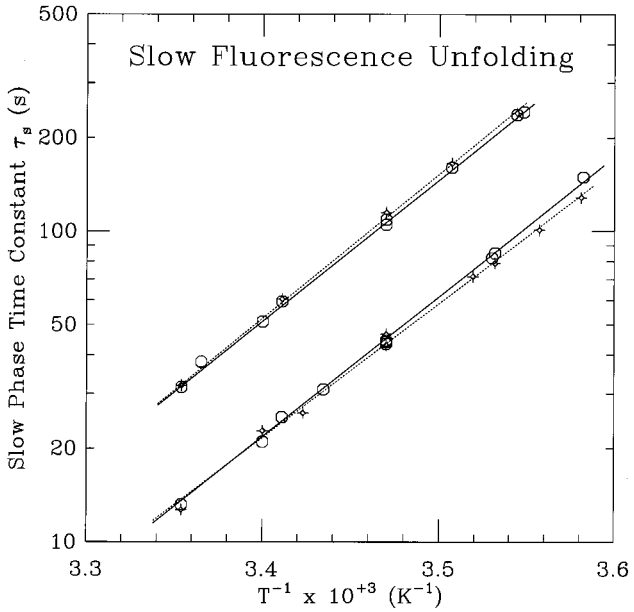

FIGURE 2: Arrhenius plots for the slow fluorescence unfolding phase of the mutants P93A (lower curve, diamonds), Y92F (lower curve, circles), P114A (upper curve, diamonds), and Y115F (upper curve, circles). The activation energies equal 19.7 ± 0.5 kcal/mol (P93A), 20.6 ± 0.4 kcal/mol (Y92F), 21.2 ± 0.5 kcal/mol (P114A), and 20.8 ± 0.3 kcal/mol (Y115F), within 95% confidence limits. The striking agreement between the data for P93A and Y92F and between the data for P114A and Y115F strongly supports the hypothesis that Y92 and Y115 report on the isomerizations of only P93 and P114, respectively (see text).

out" without affecting the ability of tyrosines to report on other processes.

The P42A mutation does not affect the slow fluorescence unfolding phase (Table 2). This is expected by the locality assumption, since Pro42 is distant from Tyr92 and Tyr115; its closest connection is through the Cys40−Cys95 disulfide bridge. As a further check, this disulfide bridge was eliminated in the [C40A/C95A] mutant (*35*), removing the close covalent linkage between Pro42 and Tyr92. The slow fluorescence unfolding phase was not significantly affected (data not shown). The Lys41−Pro42 peptide bond is *trans* in the native state (*11*), and it may be that Pro42 does not isomerize significantly to *cis* under unfolding conditions (*36*) since experiments on peptides and other proteins indicate that a Lys−Pro peptide bond remains overwhelmingly *trans* under unfolding conditions (*7*, *37*). A similar argument will be made below concerning the Lys113-Pro114 peptide group in guinea pig ribonuclease A.

The P117A mutation also does not significantly affect the slow fluorescence unfolding phase (Table 2), despite its proximity to Tyr115. However, since Pro117 is more distant from a tyrosine than prolines 93 and 114, its isomerization signal is apt to be small. Therefore, it is important to eliminate the signals from the other prolines, which might otherwise dominate the Pro117 signal. The double mutant [Y92F/P114A] was prepared; the contribution of Pro117 through Tyr115 should be readily apparent, since Tyr92 has been eliminated and Ala114 does not isomerize. However, this mutant exhibits no slow fluorescence unfolding phase, indicating that the isomerization of Pro117 is silent in the wild-type protein.

By contrast, the P114A mutation significantly alters the slow fluorescence unfolding phase (Table 2). The slow fluorescence phase of this mutant protein has a time constant of 115 ± 6 s and an activation energy of 21.2 ± 0.5 kcal/mol, which agree closely with the values for the Y115F mutant (Table 2, Figure 2). As determined by X-ray crystallography (*29*), the mutant X-Ala114 peptide bond is *trans* and causes only minor structural changes confined to residues 110−118. Thus, the isomerization of Pro114 can be selectively eliminated without perturbing the isomerizations of the other prolines.

The P93A mutation likewise alters the slow fluorescence unfolding phase significantly. The time constant of the residual slow phase is 47 ± 2 s and its activation energy is 19.7 ± 0.5 kcal/mol, which agree closely with the values measured for the Y92F mutant (Table 2, Figure 2). The situation for the P93A mutant is complicated by the fact that Ala93 may be *cis* in the folded state (*13*, *30*). This is surprising since non-prolyl *cis* residues are extremely rare (*6*) and suggests that strong *nonlocal* interactions are acting on Ala93, although the nature of these interactions remains to be determined. Fortunately, Ala93 isomerizes to *trans* much more quickly than a proline; this isomerization is essentially complete before the residual slow unfolding fluorescence phase has progressed significantly (*13*). Thus, the isomerization of the Tyr92-Ala93 peptide group does not seem to contribute to the slow unfolding fluorescence phase, *which is due to the isomerization of Pro114 in this mutant*.

Thus, it has been shown that only tyrosines 92 and 115 and only prolines 93 and 114 contribute to the slow fluorescence unfolding phase. The time constants and amplitudes of Y92F and P93A agree over a wide range of temperatures (Figure 2) and experimental conditions (Tables 2 and 3), as do the Y115F and P114A mutants. The activation energies also agree and are consistent with proline *cis*−*trans* isomerization (*4*). We therefore conclude that tyrosine 92 reports on the isomerization of proline 93 and tyrosine 115 reports on the isomerization of proline 114.

The New "Box" Model. A new box model had been proposed recently relating the eight isomeric states of the three essential prolines with the five observed *refolding* phases (*14*). This box model was determined by exhaustive statistical fitting and indicated that, under the present unfolding conditions (4.2 M Gdn·HCl, 15 °C, pH 2.0), Pro114 isomerizes with a time constant of 36 ± 3 s, Pro93 at 115 ± 7 s, and Pro117 at 17 ± 1 s (Table 7A of ref *14*). These values agree with the time constants determined from the slow fluorescence unfolding phases, which indicate that Pro114 isomerizes with a time constant of 44 ± 1 s and Pro93 at 115 ± 6 s. Such independent verification strongly suggests that the newly proposed box model is correct.

Comparison with Homology Studies. It has long been believed that Tyr92 is the only tyrosine involved in the slow fluorescence unfolding phase (*15*−*19*). The primary evidence for this was derived from homologous proteins. In particular, guinea pig ribonuclease A which has phenylalanine in place of Tyr92 exhibits no slow fluorescence unfolding phase, although it possesses the Pro114-Tyr115 peptide group. This observation poses a challenge to the "two-proline" interpretation of our results.

The amino acid sequence provides the most likely explanation for this discrepancy. Pro114 is preceded by

Asn113 in bovine pancreatic RNase A, but by Lys113 in the homologous guinea pig protein. As mentioned above, the Lys−Pro peptide bond is overwhelmingly *trans* in the unfolded state (*7*, *37*). Thus, if the Lys113−Pro114 peptide bond were *trans* in the native state of guinea pig ribonuclease A, little isomerization would occur upon unfolding, and thus the slow fluorescence phase would be absent. However, this explanation remains hypothetical, since the *cis*:*trans* ratio of Pro114 has not been measured in native or unfolded guinea pig ribonuclease A.

CONCLUSIONS

It has been shown conclusively that the slow fluorescence unfolding phase of RNase A arises from two sources: Tyr92 reporting on the *cis*−*trans* isomerization of the Tyr92-Pro93 peptide group and Tyr115 reporting on the corresponding isomerization of Pro114. The isomerizations of Pro117 and Pro42 seem to be silent by fluorescence, although earlier studies have suggested that the Lys41-Pro42 peptide group may not isomerize significantly even under unfolding conditions (*36*). The rate constants measured for the isomerizations of Pro93 and Pro114 agree closely with those determined in the recently proposed new "box" model of proline isomerization under unfolding conditions (*14*).

The site-directed mutants used in this paper enable the isomerization of *individual* X-Pro peptide groups to be monitored under unfolding conditions. It is possible to extend this type of assay to isomerizations occurring under folding conditions, using a double-jump method. In such an approach, the unfolded protein is first refolded for varying times before initiating unfolding. The *cis*−*trans* ratio of the various prolines at the moment when unfolding is initiated can be measured from the amplitudes of the respective slow unfolding phases. Such experiments are now underway in our laboratory.

The ability to measure the *cis*−*trans* isomerization of individual prolines provides a new assay for structural information on proteins in solution. The equilibrium and time constants of this isomerization may be sensitive to the local conformational structure and interactions; thus, measurements of proline isomerization may give information about the latter. In particular, changes in the equilibrium constant may monitor the development or destruction of local conformational structure. Moreover, the two states, *cis* and *trans*, are well-defined in conformation, and their observed equilibration can be used as a benchmark for comparison with molecular simulations (*38*, *39*), since the peptide dihedral angle ω provides a well-defined reaction coordinate, similar to earlier studies on tyrosine ring flipping (*40*). Such studies are underway in our laboratory.

ACKNOWLEDGMENT

We thank E. K. Fridriksson, M. Iwaoka, M. A. McDonald, M. Narayan, and T. W. Thannhauser for suggestions and assistance throughout this study and the Cornell Theory Center for computer resources. The Cornell Theory Center is funded in part by the National Science Foundation, the State of New York, the IBM Corp., and members of the Corporate Research Institute, as well as by special support for the Parallel Processing Resource for Biomedical Scientists from the National Center for Research Resources of the National Institutes of Health.

REFERENCES

1. Brandts, J. F., Halvorson, H. R., and Brennan, M. (1975) *Biochemistry 14*, 4953−4963.
2. Nall, B. T. (1994) in *Mechanisms of Protein Folding* (Pain, R. H., Ed.) pp 80−103, IRL Press, Oxford.
3. Zimmerman, S. S., and Scheraga, H. A. (1976) *Macromolecules 9*, 408−416.
4. Grathwohl, C., and Wüthrich, K. (1981) *Biopolymers 20*, 2623−2633.
5. LaPlanche, L. A., and Rogers, M. T. (1964) *J. Am. Chem. Soc. 86*, 337−341.
6. Stewart, D. E., Sarkar, A., and Wampler, J. E. (1990) *J. Mol. Biol. 214*, 253−260.
7. Raleigh, D. P., Evans, P. A., Pitkeathly, M., and Dobson, C. M. (1992) *J. Mol. Biol. 228*, 338−342.
8. Schmid, F. X., and Baldwin, R. L. (1978) *Proc. Natl. Acad. Sci. U.S.A. 75*, 4764−4768.
9. Kim, P. S., and Baldwin, R. L. (1990) *Annu. Rev. Biochem. 59*, 631−660.
10. Neira, J. L., and Rico, M. (1997) *Folding Des. 2*, R1−R11.
11. Wlodawer, A., Svensson, L. A., Sjölin, L., and Gilliland, G. L. (1988) *Biochemistry 27*, 2705−2717.
12. Koradi, R., Billeter, M., and Wüthrich, K. (1996) *J. Mol. Graph. 14*, 51−55.
13. Dodge, R. W., and Scheraga, H. A. (1996) *Biochemistry 35*, 1548−1559.
14. Juminaga, D., Wedemeyer, W. J., Garduño-Júarez, R., McDonald, M. A., and Scheraga, H. A. (1997) *Biochemistry 36*, 10131−10145.
15. Rehage, A., and Schmid, F. X. (1982) *Biochemistry 21*, 1499−1505.
16. Schmid, F. X., Grafl, R., Wrba, A., and Beintema, J. J. (1986) *Proc. Natl. Acad. Sci. U.S.A. 83*, 872−876.
17. Schmid, F. X. (1986) *FEBS Lett. 198*, 217−220.
18. Lin, L.-N., and Brandts, J. F. (1987) *Biochemistry 26*, 1826−1830.
19. Lin, L.-N., and Brandts, J. F. (1988) *Biochemistry 27*, 9037−9042.
20. Rothwarf, D. M., and Scheraga, H. A. (1993) *Biochemistry 32*, 2671−2679.
21. Sambrook, J., Fritsch, E. F., and Maniatis, T. (1989) *Molecular Cloning*: *A Laboratory Manual*, Cold Spring Harbor Laboratory Press, New York.
22. Thannhauser, T. W., Konishi, Y., and Scheraga, H. A. (1987) *Methods Enzymol. 143*, 115−119.
23. Denton, J. B., Konishi, Y., and Scheraga, H. A. (1982) *Biochemistry 21*, 5155−5163.
24. Crook, E. M., Mathias, A. P., and Rabin, B. R. (1960) *Biochem. J. 74*, 234−238.
25. Nozaki, Y. (1972) *Methods Enzymol. 26*, 43−50.
26. Santoro, M. M., and Bolen, D. W. (1988) *Biochemistry 27*, 8063−8068.
27. Houry, W. A., Rothwarf, D. M., and Scheraga, H. A. (1994) *Biochemistry 33*, 2516−2530.
28. Press, W. H., Teukolsky, S. A., Vetterling, W. T., and Flannery, B. P. (1992) *Numerical Recipes in C*, 2nd ed., Cambridge University Press, Cambridge.
29. Schultz, D. A., Friedman, A., and Fox, R. O. (1993) *Protein Sci. 2* (Suppl. 1), 67.
30. Pearson, M. A., Karplus, P. A., Dodge, R. W., Laity, J. H., and Scheraga, H. A. (1998) *Protein Sci. 7*, 1255−1258.
31. Richards, F. M., and Wyckoff, H. W. (1971) *Enzymes 4*, 647−806.
32. Sendak, R. A., Rothwarf, D. M., Wedemeyer, W. J., Houry, W. A., and Scheraga, H. A. (1996) *Biochemistry 35*, 12978−12992.
33. Mui, P. W., Konishi, Y., and Scheraga, H. A. (1985) *Biochemistry 24*, 4481−4489.

34. Shimotakahara, S., Ríos, C. B., Laity, J. H., Zimmerman, D. E., Scheraga, H. A., and Montelione, G. T. (1997) *Biochemistry 36*, 6915−6929.
35. Laity, J. H., Lester, C. C., Shimotakahara, S., Zimmerman, D. E., Montelione, G. T., and Scheraga, H. A. (1997) *Biochemistry 36*, 12683−12699.
36. Dodge, R. W., Laity, J. H., Rothwarf, D. M., Shimotakahara, S., and Scheraga, H. A. (1994) *J. Protein Chem. 13*, 409−421.
37. Dyson, H. J., Rance, M., Houghten, R. A., Lerner, R. A., and Wright, P. E. (1988) *J. Mol. Biol. 201*, 161−200.
38. Pincus, M. R., Gerewitz, F., Wako, H., and Scheraga, H. A. (1983) *J. Protein Chem. 12*, 131−146.
39. Chandler, D. (1978) *J. Chem. Phys. 68*, 2959−2970.
40. Northrup, S. H., Pear, M. R., Lee, C.-Y., McCammon, J. A., and Karplus, M. (1982) *Proc. Natl. Acad. Sci. U.S.A. 79*, 4035−4039.

BI981028E